Tests on Some Programmed Numerical Wave Forecast Models

P. E. DEXTER

Bureau of Meteorology, Melbourne, Australia

(Manuscript received 18 March 1974, in revised form 28 June 1974)

ABSTRACT

Numerical forecasting of wind-generated ocean waves by digital computer may be attempted using any of three fundamentally different ways of describing wave generation and decay: empirical significant wave, empirical spectral, and theoretical spectral. This paper describes four models, covering the three types, which have been programmed with a view to the adaptation of one or more into a numerical wave forecast system for the Australian region. Results from a simple test situation are presented, both for comparison purposes and as a check on the internal consistency of the model's generation and decay functions.

1. Introduction

The past 20 to 30 years have seen a considerable upsurge in research activity in the field of wind-generated ocean waves—their description, generation and decay. This research has been prompted both by the availability of increasingly sophisticated techniques for measuring sea waves and then handling the considerable volume of data so obtained, and by an increasing demand by both government and commercial interests for reliable data on past (climatological) and future (forecast) sea states.

In response to this demand, a number of different techniques have been developed for hindcasting or forecasting sea waves which result from given surface wind fields. Initially these techniques were manual, requiring the services of a skilled "wave forecaster," but the need to provide forecast (hindcast) data over large ocean areas, the desire to remove the subjectivity inherent in manual methods, the general amenability of wave generation and decay functions to numerical computational methods, and the continued improvement in computing capabilities, have all led to the further development of numerical wave forecast (hindcast) models.

In general, these numerical models may be classified according to both the parameters they use to describe sea states, and the methods they adopt to assess quantitatively wave growth and decay. Thus we may have "empirical significant wave models," which compute significant wave heights and periods using empirical growth and decay functions; "empirical spectral models," which also use empirical formulas to describe the growth and decay of wave spectra; and "theoretical spectral" models, which compute the total response of sea wave spectra to surface wind fields using the most recent theories on energy transfer, both from wind to waves and within the wave spectra themselves.

Within these three classifications a number of models have been developed to meet differing requirements: for example, large-scale deep-water forecasts for shipping; nearshore forecasts for fishing and recreational interests; point-climatologies of sea states for coastal engineering purposes; and forecasts of extreme wave conditions, necessary for shore protection and civil defense. The Australian Bureau of Meteorology is presently engaged in the development of a comprehensive sea-state information system, which will incorporate one or more numerical wave models, and in line with this overall project some ten different published models have been summarized and compared (Dexter, 1973), together with another empirical spectral model that has been formulated by the author.

Altogether, four of these models (one empirical significant wave, one empirical spectral, and two theoretical), with certain modifications, have been programmed. The models as programmed are outlined in this paper, their results compared on the basis of a simple comparison and consistency test, and their likely performance in real-time forecast or hindcast situations assessed.

The effects of atmospheric stability on wave generation are not well understood (Cardone, 1969), but are probably significant. Nevertheless, no attempt has been made, as yet, to introduce these effects into the programmed models explicitly, and it is assumed that all generation occurs under conditions of neutral stability. In addition, the surface wind is assumed defined at a height of 19.5 m above the still-water level, as recommended by Pierson (1964), unless otherwise stated.

2. The models

All empirical significant wave forecast models depend on empirical formulas relating significant wave height to wind speed and fetch or duration. These include the empirical relationships between dimensionless parameters (gH_s/U^2), (gF/U^2) and (C_s/U), originally proposed by Wilson (1955, 1961) to fit the available data:

$$\left.\begin{aligned} gH_s/U^2 &= 0.26 \tanh[(1/10^2)(gF/U^2)^{\frac{1}{2}}] \\ C_s/U &= 1.40 \tanh[(4.36/10^2)(gF/U^2)^{\frac{1}{3}}] \end{aligned}\right\}, \quad (1)$$

where H_s is significant wave height, U surface (10 m level) wind speed, F fetch length, g gravity, and C_s deep water propagation speed of the "significant waves." More recently, expressions of the same kind as (1) have been advocated by Wilson (1965) and adopted by Wilson *et al.* (1973) and Feldhausen *et al.* (1973). On the other hand, both empirical spectral and theoretical spectral models make use of the energy balance equation

$$\partial E(\omega,\theta,\mathbf{x},t)/\partial t = -\mathbf{C}_g \cdot \nabla E(\omega,\theta,\mathbf{x},t) + S(\omega,\theta,\mathbf{x},t), \quad (2)$$

where $E(\omega,\theta,\mathbf{x},t)$ is wave energy density (actually the contribution to the variance of sea surface displacement) of the spectral component at circular frequency ω and direction θ, at the space-time position $\mathbf{x},t$; $\mathbf{C}_g$ is the deep water group velocity appropriate to that component; and $S(\omega,\theta,\mathbf{x},t)$ is termed the source function, also for that spectral component at the relevant position. For empirical spectral models, S may represent an empirical growth and/or decay function for wind waves, while for theoretical spectral models it contains representations of all processes which add energy to, or subtract energy from, the spectrum. The first term on the right-hand side of (2) represents swell propagation. The use of this equation in numerical wave forecast models was proposed, independently, by Gelci *et al.* (1956), Hasselmann (1960) and Groves and Melcer (1961), and has been adopted by a number of different workers since then (e.g., Barnett, 1968; Ewing, 1971).

a. The Wilson-Trajer model

This model is an adaptation by Trajer (1966) of the numerical "wave ray" approach suggested by Wilson (1961, 1963). It is designed to provide a time history or forecast of significant wave heights and periods at a target point by generating "wave packets" at fixed intervals along rays which emanate from points in a space-time field of wind velocity and then propagating and growing or decaying these packets down the rays to the target point. It is particularly suited for use with such well-defined and limited space-time wind fields as are associated with tropical cyclones, where the resulting time history of wave heights at a specified point is required, for example, for design or civil defense. Nevertheless, the model may also be used with any other type of properly defined wind field, and its results thus compared, in some limited way, with results from the other models outlined in this paper.

The basic wave generation equations employed by the model are just approximations to (1), valid for small fetch increments:

$$\left.\begin{aligned} gH_s/U^2 &\approx 0.40/10^2(g\Delta F/U^2)^{0.40} \\ C_s/U = gT_s/2\pi U &\approx 8.00/10^2(g\Delta F/U^2)^{0.26} \end{aligned}\right\}, \quad (3)$$

where T_s is the significant wave period, and ΔF the fetch increment along the rays. The constants of (1) have been altered slightly in (3) so as to give greater accuracy for the small fetch increments used.

The model assumes that wave packets propagate with fixed period over any given time or space step, the propagation velocity being just $C_g = C_s/2 = gT_s/4\pi$. Wave decay has been incorporated by digitizing the Bretschneider (1952) decay curves, with decayed wave height then obtained by interpolation.

The spatial grid is defined by rays emanating from the target point at angular increments of 15° through any required segment (or a full 360°). Grid points are located at fixed intervals along these rays, these intervals being chosen such that the stability criterion $C_g > \lambda/\tau$ (λ = space increment, τ = time increment) is satisfied for all wave periods of interest.

Over this grid, the wind field is then defined every 3 hr, and wind vector components along the rays toward the target point computed. Wave packets are generated by these components and propagated (with growth or decay, depending on subsequent wind speeds) down the rays to the target. The heights and periods of wave packets reaching the target point are plotted against time of arrival, and the envelope of plotted points represents the time history of significant waves at the target.

In general, the approach adopted in this model is probably the best that can be achieved using only the significant wave as a description of sea state.

b. An empirical spectral model

All empirical spectral models depend essentially on formulations for the source function S in (2) in terms of an empirical wave growth function, a limiting spectral form, and, if necessary, some empirical decay term. In this particular model these terms are as follows:

(i) Spectral growth is computed according to the relationship derived by Pierson *et al.* (1965) (given in Blumenthal *et al.*, 1967), giving the total spectral variance $[\sigma^2]$ as a function of wind speed U and duration t:

$$[\sigma^2] = 4.067 \times 10^{-3} U^2 [\exp(0.103t) - 1], \quad (4)$$

where $[\sigma^2]$ is in meters², U in meters per second, and t in hours.

(ii) The fully-developed one-dimensional spectrum of Pierson and Moskowitz (1964), together with the angular spreading factor of Neumann (1952), is employed for the limiting wind wave spectrum, i.e.,

$$E(\omega,\phi)d\omega d\phi = (2\alpha g^2/\pi\omega^5) \times \exp[-\beta(g/U\omega)^4] \cos^2\phi \, d\omega d\phi, \quad (5)$$

where ϕ is the angle between wind and wave directions, and α,β are nondimensional constants (8.1×10^{-3} and 0.74, respectively). MKS units are used for E, g, ω, U. This may be integrated over $\omega(0$ to $\infty)$ and $\phi(-\pi/2$ to $+\pi/2)$ to give total spectral energy E_T:

$$E_T=[\sigma^2]=\alpha U^4/(4\beta g^2). \qquad (6)$$

Total wave energy is then

$$E_s=2[\sigma^2]=\alpha U^4/(2\beta g^2). \qquad (7)$$

(iii) Following Bunting (1966), his additional empirical dissipation function has been introduced here to give a better representation of wave component decay, particularly for opposing winds:

$$E_D(\omega,\theta)=E_I(\omega,\theta)[\exp\{-C'\omega^4E_T^{0.5}\}]^{K(\phi)}, \qquad (8)$$

where E_I, E_D are the spectral energies of a particular component before and after dissipation respectively, C' is a constant, and $K(\phi)$ is an empirical nondimensional function of ϕ.

From (4) we derive the rate of change of spectral variance for wind speed U and duration t:

$$d[\sigma^2]/dt=4.189\times10^{-4}U^2\exp(0.103t), \qquad (9)$$

and equivalent duration, t_{eq}, given variance $[\sigma^2]$ and wind speed U:

$$t_{eq}=9.709\ln\{[\sigma^2]/(4.067\times10^{-3}U^2)+1\}. \qquad (10)$$

Using some finite difference equivalent to (9), the variance increment added to the sea, $\delta[\sigma^2]_k$, during the kth time step of length δt is computed. A constant wind speed U_k is assumed throughout the step, and an equivalent duration for wind U_k during this step is obtained from (10), given the total effective wind-sea variance $[\sigma]_{k-1}$ at the end of the previous step. The value of $[\sigma^2]_{k-1}$ to be used is found by summing only those spectral components which are moving within $\pm\pi/2$ of the new wind direction. The remainder are decayed as swell according to (8).

At the end of any time step (say the kth), spectral values corresponding to total variance $[\sigma^2]_k$ are assigned by assuming that the wind-sea spectrum maintains its shape throughout the growth phase. On this basis $[\sigma^2]_k$ in (6) is used to compute an equivalent duration, U_{eq}, for a fully-developed spectrum. This value of U_{eq} is then substituted in (5) to determine spectral values. If U_{eq} exceeds the wind speed U_k during the kth step, then $[\sigma^2]_k$ is reduced to its fully developed value corresponding to U_k, and the wind-sea grows no further.

Unfortunately, as has been pointed out by Pierson (reported in Blumenthal *et al.*, 1967), Eq. (4) gives too rapid wave growth in both the initial and final stages of development, probably because the wave data from which it was derived were contaminated with propagated wave energy. It is necessary to remove the effects of the contamination and this has been done here, empirically, by following Pierson's suggestions for estimating actual durations of wave growth. This approach certainly gives realistic results for the simple test conditions described in the next section, but may not work so well with more complex wind fields, requiring some further model refinements.

To describe the energy spectrum in the model, the frequency domain was divided into 19 bands, centered on 1/4, 1/5, 1/6, . . . 1/22 Hz, and direction of propagation into 12 sectors, each of 30°, giving a total of 228 spectral components. Some saving in computation time has been effected by assuming full spectral development to occur instantaneously at frequencies above $\frac{1}{6}$ Hz, with these same components decaying to zero immediately the wind drops. This procedure also helps to preserve computational stability at the higher frequencies, while not seriously affecting results, especially in the important strong-wind situations. A time step of 1 hr has been accepted as the best compromise between computational stability, and wind field definition. In real-time forecast situations it may be necessary to reduce the spectral definition, particularly in the frequency domain, so that the total number of components does not exceed about 100. This is to further conserve machine time, and should not reduce the low-frequency resolution significantly.

c. *The Inoue model*

This may be termed a theoretical spectral model, since it is based on (2), and the source function S is composed of quantitative representations of the wave growth theories of Miles (1957) and Phillips (1957, 1966), together with an empirical damping term which allows for the smooth transition of the wave spectrum to an equilibrium of fully-developed state. The model equations were developed originally by Inoue (1967), and a full working model, together with results from forecast tests, was outlined by Bunting (1970).

The programmed version of the model is essentially that described by Bunting. The fully-developed state is the Pierson-Moskowitz (1964) spectrum, and the model's performance has been improved under variable wind conditions by including Bunting's (1966) empirical decay function (8). The linear and exponential growth terms of Inoue, based on the theories of Phillips and Miles, respectively, have been included unchanged. The model's principal inadequacies are the lack of any representations for the processes of wave breaking (Phillips, 1958), and nonlinear wave-wave interactions (Hasselmann, 1962), both of which are important to the growth and maintenance of the full wave spectrum.

The same components have been used to describe the energy spectrum as were discussed with the previous model, and the time step in the integrations has again been set at 1 hr. Basically, this model has been programmed and tested, despite its inadequacies, because its simplicity allows for relatively rapid solutions, a distinct advantage when real-time wave forecasts are required. The results are of acceptable accuracy in simple test situations, but may be of less value with more complex wind fields.

d. The Barnett model

The general form of the model proposed by Barnett (1968) would seem to be the most comprehensive available at the present time. It is likely that changes will be made in the detailed specifications for individual terms in the model equation as theories on the growth and decay of wave spectra advance, and better experimental data become available. However, the model form should remain largely unchanged for some time.

Once again (2) is the basis for the model, with the source function S now composed of the following terms: (i) linear growth term A, based on the resonance theory of Phillips (1957); (ii) exponential growth term B, related to the work of Miles (1957) and Phillips (1966), but in this case derived in a purely empirical way; (iii) damping term $(1-D)$, being some representation of the process of wave breaking (Phillips, 1958); and (iv) wave-wave interaction term $(\Gamma-\tau E)$ involving a parameterization of the theoretical formulations of Hasselmann (1962, 1963). Thus, the full energy balance equation is now

$$\partial E/\partial t=-\mathbf{C}_g\cdot\nabla E+(A+BE)(1-D)+(\Gamma-\tau E). \qquad (11)$$

In the programmed version of this model, some minor changes in details of the source function terms have been made in order that these terms give an improved fit to experimental data. These changes include: 1) $A\propto U^{1.75}$, compared with Barnett's $A\propto U^{3.75}$ and Inoue's $A\propto U^{2.25}$ (in practice, this change is of little importance since the A term has an influence only in the initial generation of waves, and its effects are soon overtaken by those of the B term); 2) an empirical specification of the B term which is a slightly more realistic fit to the same experimental data; and 3) the choice of

$$E(\omega,\phi)=(2\pi\ 8.1\times10^{-3}g^2/\omega^5)8\cos^4\phi/3\pi \qquad (12)$$

(after Pierson and Moskowitz, 1964) to represent the equilibrium range at the high-frequency end of the wave spectrum. This is important in controlling spectral energy values, through the damping factor D.

A model very similar to that of Barnett has been published by Ewing (1971), and the changes outlined above are in line with details of Ewing's model. In addition, in order to avoid computational instabilities at high wave frequencies, to decrease computation time, and because the high-frequency components will generally be of little interest in most applications of wave forecasts, the spectrum has been assumed in equilibrium at all times above a certain frequency, which has been set as a function of wind speed as follows:

$U=0$, for $f\geqslant0.16$ sec^{-1}, $E(f)=0$

$U\leqslant15$ m sec^{-1}, for $f\geqslant0.16$ sec^{-1}, $E(f)=$ equilibrium value

$15<U\leqslant25$ m sec^{-1}, for $f\geqslant0.12$ sec^{-1}, $E(f)=$ equilibrium value

$U>25$ m sec^{-1}, for $f\geqslant0.11$ sec^{-1}, $E(f)=$ equilibrium value

The equilibrium value is computed from the equilibrium range spectrum (12).

The programmed version of Barnett's model has the same frequency and angle components to describe the wave spectrum as are employed in the other two spectral models programmed. The numerical integration of the source function part of (11) has been carried out using a fourth-order Runge-Kutta technique with a time step of 1 hr. This is certainly too slow to be considered in a practical situation, and will be replaced by either a second-order Runge-Kutta, or (more likely) a predictor-corrector technique.

3. Some test results

For convenience in this and the following section, and in the diagrams, the various programmed models are designated as: (i) significant wave model developed by Trajer using the method of Wilson [W-T]; (ii) spectral model described here, with the decay term of Bunting [D-B]; (iii) spectral model of Inoue, as used by Bunting: [I-B]; (iv) spectral model of Barnett [B].

In order to establish the internal consistency of these models, and to provide a means of comparing their results, a simple test situation has been applied. A wind of 15 m sec^{-1} (at a height of 10 m) was introduced instantaneously over a calm sea and allowed to blow in a constant direction for 30 hr, after which time it was reduced to zero and the developed wave field decayed for a further 30 hr under the influence of the model damping terms. These conditions were applied uniformly over the whole of the spatial field, so that the effects of both wind fetch and the propagation term in (2) were essentially ignored, at least in the three spectral models. Thus for these three models the responses of the relevant source functions to the same duration-limited wind field, only, were considered. Because the propagation term is identical in the three models this then provides an effective means of comparing total model response to the simple wind field, in addition to testing the internal consistency of the source functions. The situation for model W-T is somewhat different, both because of the special nature of the spatial grid, and because of the form of the empirical growth and decay functions. Nevertheless, it should still be possible to compare results from this

TABLE 1. Full (two-dimensional) spectrum of model D-B after 30 hr growth with 15 m sec^{-1} wind. Spectral values have units of m^2 sec rad^{-1}.

Direction from (deg)	Period (sec) 4	5	6	7	8	9	10	11	12	13	14	15	16	17	18	19	20	21	22
180	0.0	0.0	0.0	0.0	0.0	0.0	0.0	0.0	0.0	0.0	0.0	0.0	0.0	0.0	0.0	0.0	0.0	0.0	0.0
210	0.0	0.0	0.0	0.0	0.0	0.0	0.0	0.0	0.0	0.0	0.0	0.0	0.0	0.0	0.0	0.0	0.0	0.0	0.0
240	0.0	0.0	0.0	0.0	0.0	0.0	0.0	0.0	0.0	0.0	0.0	0.0	0.0	0.0	0.0	0.0	0.0	0.0	0.0
270	0.0	0.0	0.0	0.0	0.0	0.0	0.0	0.0	0.0	0.0	0.0	0.0	0.0	0.0	0.0	0.0	0.0	0.0	0.0
300	0.00	0.07	0.31	0.82	1.65	2.72	3.85	4.70	4.97	4.51	3.48	2.24	1.18	0.50	0.17	0.04	0.01	0.00	0.00
330	0.01	0.20	0.93	2.47	4.95	8.17	11.54	14.10	14.91	13.54	10.43	6.71	3.54	1.50	0.50	0.13	0.02	0.00	0.00
360	0.01	0.27	1.24	3.30	6.60	10.89	15.38	18.80	19.88	18.06	13.91	8.94	4.72	2.00	0.66	0.17	0.03	0.00	0.00
30	0.01	0.20	0.93	2.47	4.95	8.17	11.54	14.10	14.91	13.54	10.43	6.71	3.54	1.50	0.50	0.13	0.02	0.00	0.00
60	0.00	0.07	0.31	0.32	1.65	2.72	3.85	4.70	4.97	4.51	3.48	2.24	1.18	0.50	0.17	0.04	0.01	0.00	0.00
90	0.0	0.0	0.0	0.0	0.0	0.0	0.0	0.0	0.0	0.0	0.0	0.0	0.0	0.0	0.0	0.0	0.0	0.0	0.0
120	0.0	0.0	0.0	0.0	0.0	0.0	0.0	0.0	0.0	0.0	0.0	0.0	0.0	0.0	0.0	0.0	0.0	0.0	0.0
150	0.0	0.0	0.0	0.0	0.0	0.0	0.0	0.0	0.0	0.0	0.0	0.0	0.0	0.0	0.0	0.0	0.0	0.0	0.0

model with those of the other three, at least in some limited sense.

The test wind of 15 m sec^{-1} has been set at a height of 10 m above still water level so as to afford consistency with more general wind fields derived from synoptic weather charts. However, this wind must be converted to an equivalent wind speed at a height of 19.5 m before it can be substituted in any of the spectral models. This has been accomplished here by assuming a (neutral stability) logarithmic wind profile, which gives

$$U_z = U_{10}[1+\ln(z/10)(C_{10})^2/\kappa], \qquad (13)$$

where U_z, U_{10} are wind speeds at heights z and 10 m, respectively, κ is von Kármán's constant, and C_{10} is the 10 m drag coefficient. With Deacon and Webb's (1962) value for C_{10}, Eq. (13) becomes

$$U_{19.5} = U_{10}[1+1.67(10^{-3}+7\times10^{-5}U_{10})^{\frac{1}{2}}]. \qquad (14)$$

For $U_{10}=15$ m sec^{-1}, the value of $U_{19.5}$ is then 16.13 m sec^{-1}. Some care has to be exercised in comparing energy values from our three spectral models with results for standard (fully-developed) spectra, which may be derived for winds at heights other than 19.5 m (Pierson, 1964).

In order to compare results from model W-T with those of the spectral models, sets of results must be given in terms of some common sea surface parameter. This is done most conveniently here by converting total spectral wave energy from the spectral models to an equivalent significant wave height. Now total spectral energy (spectral variance) is just half the total sea wave energy. Thus

$$E_s = 2E_T = 2[\sigma^2] = 2\int\int E(\omega,\theta)d\omega d\theta. \qquad (15)$$

However, from Longuet-Higgins (1952),

$$H_s = 2.83(E_s)^{\frac{1}{2}}, \qquad (16)$$

at least for a "narrow-band" wave spectrum. This last condition is certainly not true for the spectra we computed, but it is still possible to make at least a limited comparison of time histories of significant wave height obtained from the spectral models by way of (15) and (16) with those of model W-T.

Records of significant wave height and period at the target points [points $(0,t)$ in distance-time] derived in model W-T are shown in Figs. 1a and 1b. Plotted points represent wave packets arriving at the target along the various rays at different times, and a complete time history is the envelope of these points. This is the normal form of program output, and from such time histories, various climatological parameters, wave height exceedence curves, etc., may be simply derived.

The growth and decay with time of the one-dimensional energy spectrum for model D-B under the test conditions are shown in Figs. 2a and 2b, respectively. In practice, full two-dimensional spectra are computed, and as an example the full spectrum after 30 hr growth is given in Table 1. Spectral shape for this model during the growth phase is, in effect, defined by the Pierson-Moskowitz spectrum, so we would not expect Fig. 2a to exhibit any irregularities. Indeed, it also appears to be quite consistent with available experimental data on wave growth. A state of full development is attained after 23 hr, which is consistent with growth times for some of the spectra discussed by Walden (1963), and with the work of Gelci *et al.* (1956). However, if model B is correct, in particular in its parameterizations of the work of Hasselmann (1962), then the concept of a fully-developed spectrum is very much in doubt, since growth at lower frequencies will continue at all times through nonlinear interactions. In this particular test, no significant differences in spectral energies were found as a result of this process; and indeed in practice it is unlikely that major problems will arise because of the extreme durations required at most wind speeds of interest for the "fully developed" state to be significantly exceeded.

Wave decay in model D-B occurs through the Bunting (1966) decay term (8), and Fig. 2b exhibits

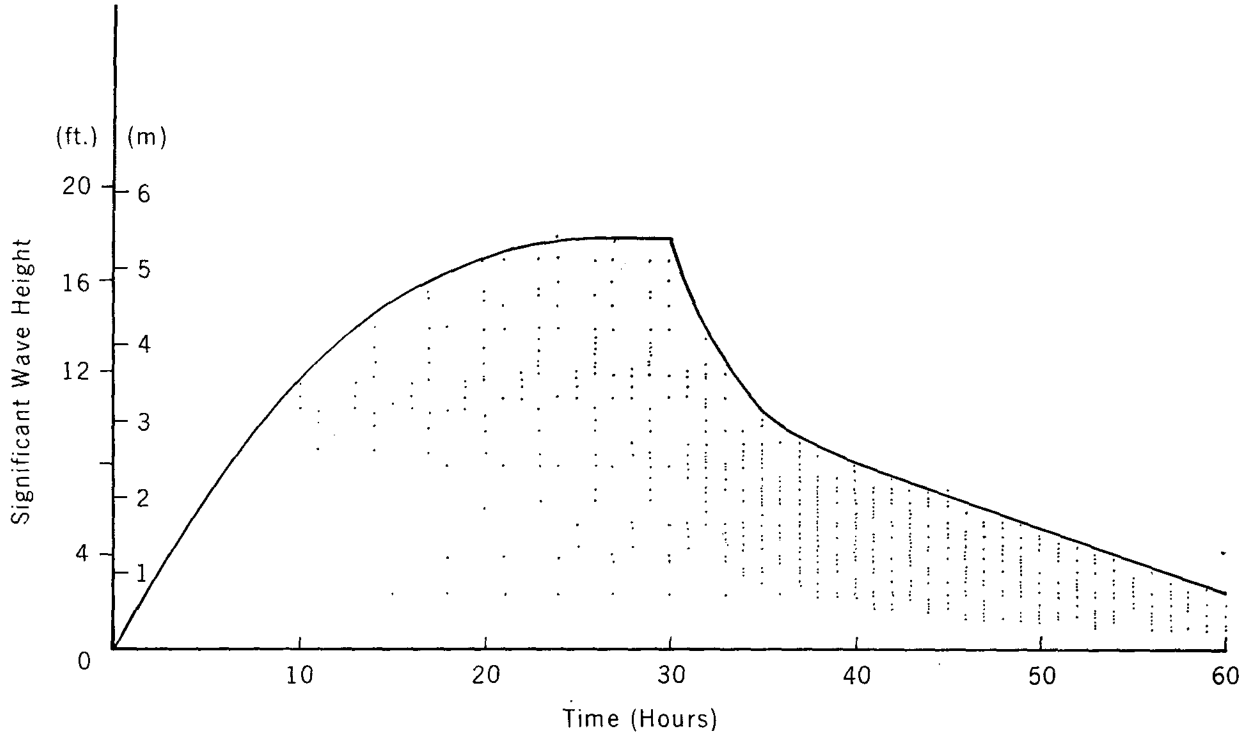

FIG. 1a. Time history of significant wave height (m) at the target points $(0,t)$ for model W-T. Wind speed is 15 m sec^{-1} (at 10 m) for time 0–30 hr, and 0 m sec^{-1} for time 30–60 hr.

the features expected of this process—rapid decay at higher frequencies, a narrowing of the spectral width, and a shift in the spectral peak toward low frequencies. It is also remarkably consistent with decay according to model B, where the process occurs through the nonlinear terms only. Similar growth and decay spectra have been computed for models I-B and B, but are not reproduced here since they essentially duplicate

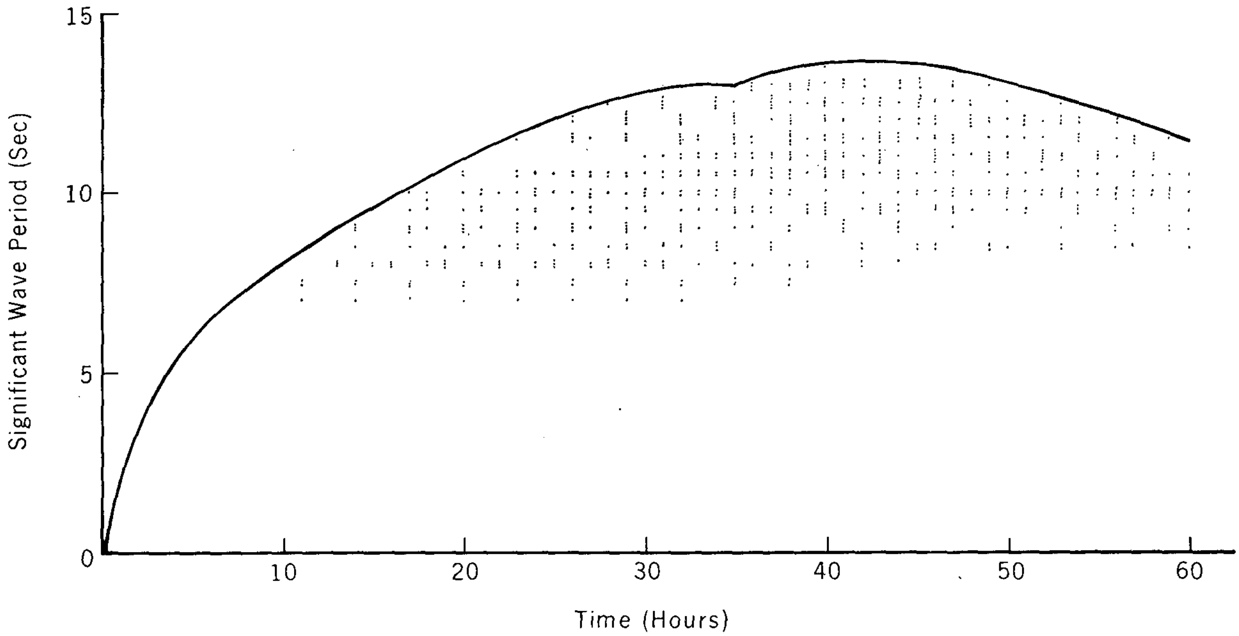

FIG. 1b. Time history of significant wave period (sec) for conditions of Fig. 1a.

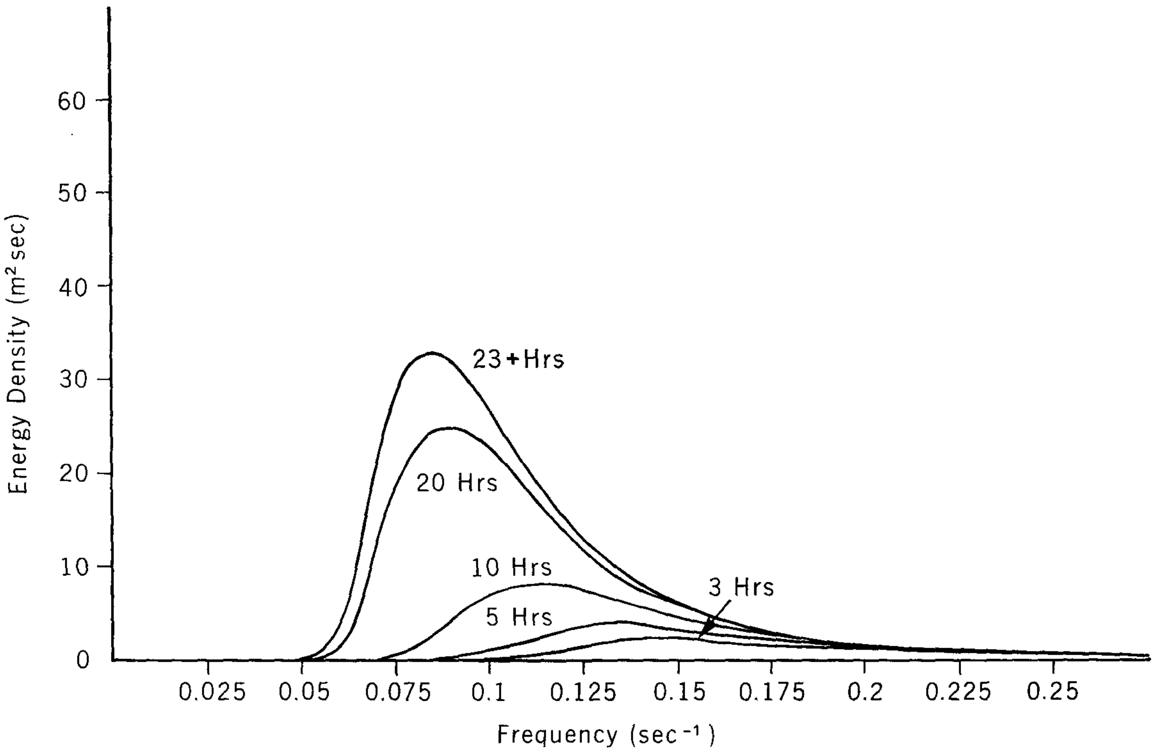

Fig. 2a. Spectral growth at a point for model D-B. Wind speed is a uniform 15 m sec^{-1} (at 10 m) over an infinite ocean.

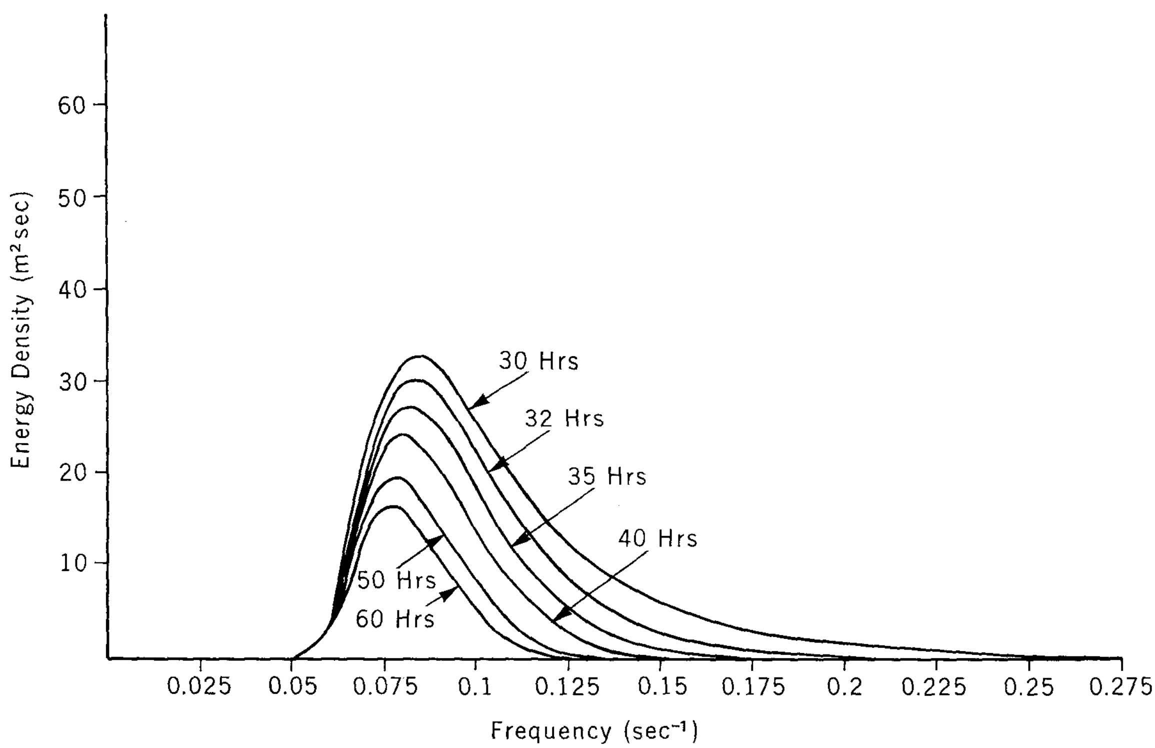

Fig. 2b. Spectral decay at a point for model D-B. Wind speed is 0 m sec^{-1}.

the published work of Inoue (1967) and Barnett (1968). The small changes we have made in Barnett's model do not appear to significantly alter spectral growth rates, or energy values, at least under these test conditions.

In order to afford a ready means of comparison for all models, we have, in Fig. 3a, plotted time histories of significant wave height through both growth and decay periods. In the case of the spectral models, equivalent significant wave heights were computed using (15) and (16); while a similar growth curve derived from Bretschneider's (1970) latest revision of the Sverdrup-Munk-Bretschneider (SMB) forecast graphs is included for comparison with model W-T. Some points concerning Fig. 3a are of interest:

1) The very rapid early growth in wave height with model B results from our stability conditions, discussed in Section 2d, and is not a "real" effect.

2) Model I-B is the first to attain a "fully developed" state (after 18 hr), and shows the most rapid increase in wave height during the middle stages of growth, from 3 to 13 hr.

3) Heights are, in general, greatest for model B throughout; and both this model and the SMB curves continue to exhibit wave growth at 30 hr duration. Significantly, the spread in wave heights among all five models after this 30 hr is less than 1 m; it is greatest, in both relative and absolute terms, after about 3 hr.

4) Models D-B and W-T exhibit remarkably similar characteristics throughout the growth period. D-B and I-B grow to the same significant wave height, since they both use the Pierson-Moskowitz spectrum as a limiting form; and their decay curves are also identical.

5) Since a finite spatial grid was used with model W-T (about 600 n mi in extent), growth is fetch-limited, which probably explains the apparent full development after 25 hr. Similarly, the continuing rapid decay in the model after about 40 hr is also fetch controlled.

6) The decay curves of models B and D-B (or I-B) are similar, but tend to diverge. This is undoubtedly a result of the effects of the nonlinear terms in model B, which allow continued wave growth at low frequencies and thus give slower decay in total spectral energy, or significant wave height.

A parameter which is of interest in any study of the processes of spectral growth and decay is the frequency at which maximum spectral energy occurs, or the spectral mode frequency f_m. This has been plotted as a function of time in Fig. 3b for each of the three models. In general, the graphs are characterized by a rapid shift in f_m to about 0.11 Hz, followed by a more gradual drift to still lower frequencies. This drift

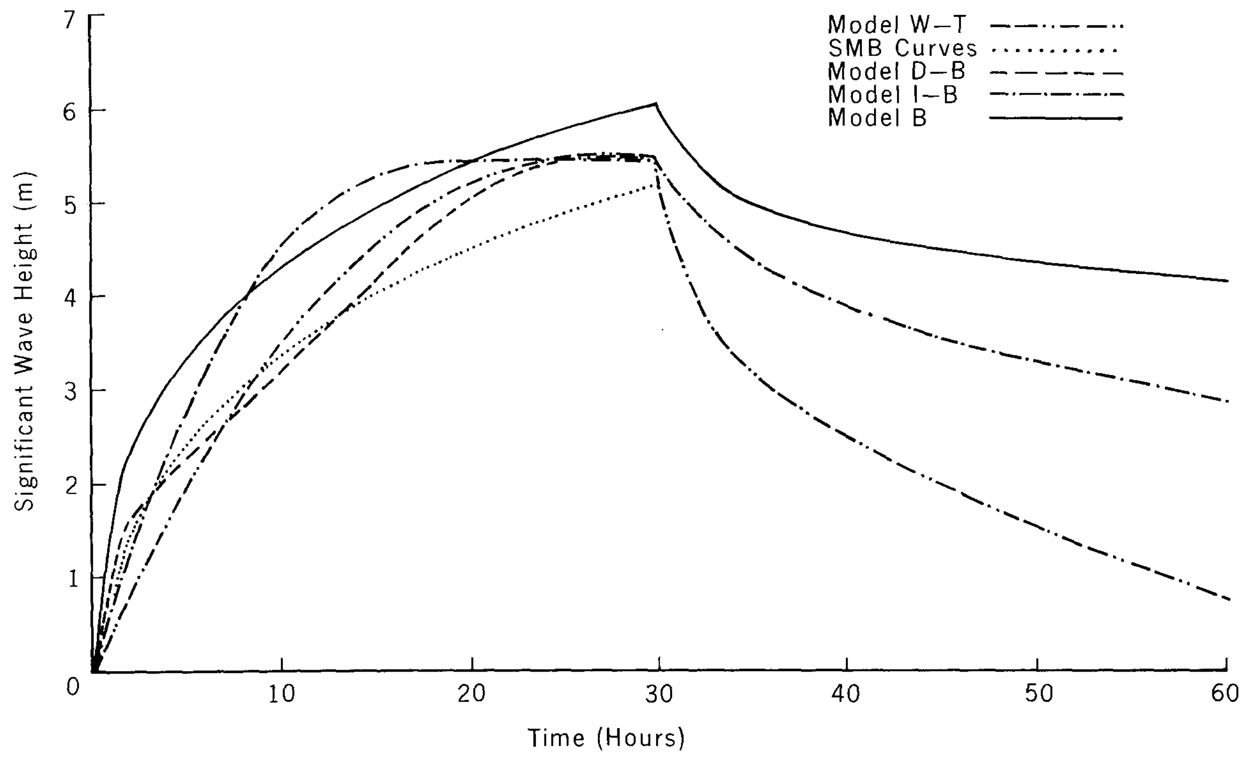

FIG. 3a. Time histories of significant wave height (m) for all models, where $U_{10}=15$ m sec^{-1} (0–30 hr) and $U_{10}=0$ (30–60 hr).

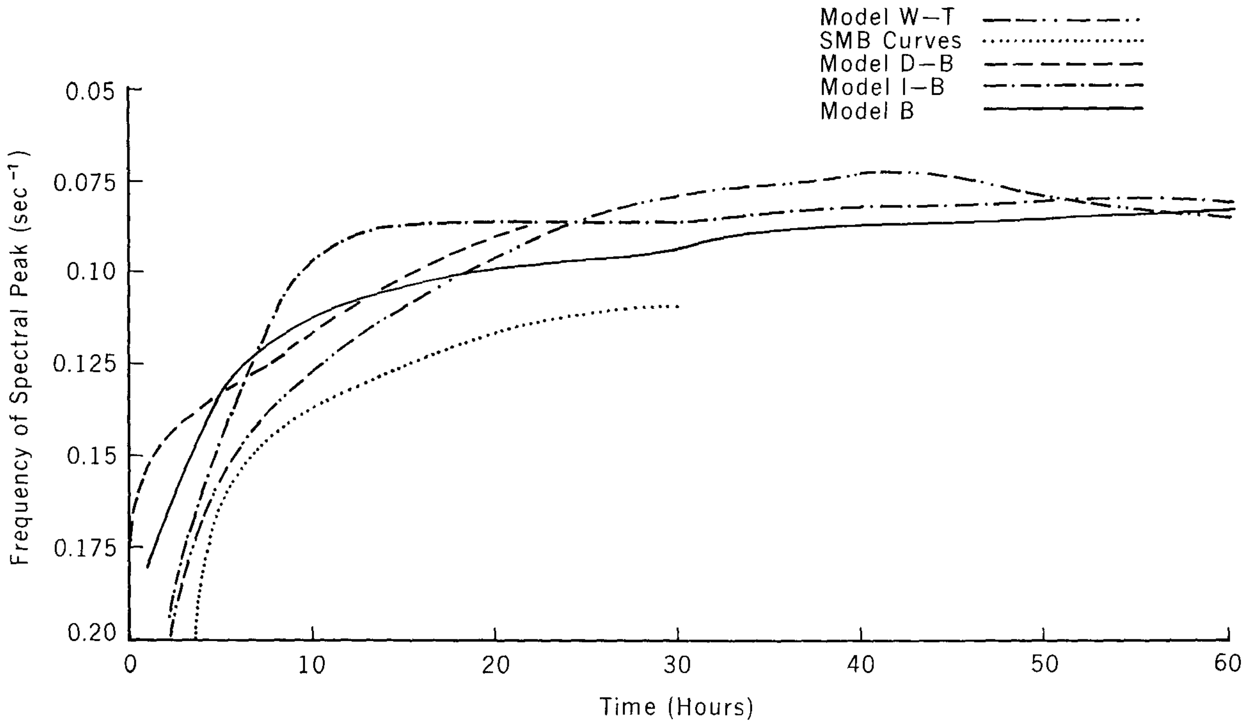

FIG. 3b. Time histories of spectral mode frequency f_m(Hz) for models D-B, I-B and B, and significant wave frequency f_s(Hz) for model W-T and the SMB curves. Wind conditions are as in Fig. 3a.

continues throughout the decay period, since higher frequencies dissipate first. Model I-B has the most rapid movement of mode frequency, while the fully-developed Pierson-Moskowitz spectrum has a lower mode than model B (after 30 hr). Also included in Fig. 3b are plots of significant wave frequency ($f_s = 1/T_s$) for model W-T, and that derived from Bretschneider's (1970) forecast curves. Interestingly, the graph for W-T lies close to that for D-B, particularly after about 10 hr growth. It would thus appear that the value of f_s computed in model W-T can provide a reasonable measure of spectral mode frequency. On the other hand, the value of f_s from Bretschneider's curves is always higher than f_m. However, if the relationship

$$(1/f_m) = 1.14(1/f_s),$$

suggested by Darbyshire (1959), is applied, the curve is shifted into quite close agreement with that of model B.

4. Conclusions

It is apparent from results of model tests to date that overall differences in product of the three spectral models are relatively slight—certainly under simple meteorological conditions. Indeed, they are almost certainly less than those arising from errors in oceanic wind fields. Of the three, the Inoue-Bunting model probably performs least well, in terms of both response to applied winds and resulting spectral values.

Perhaps surprisingly, significant wave height and period computed in the Wilson-Trajer model agree quite well with equivalent parameters derived from the three spectral models. Thus within the context of the significant wave description of the sea surface, this model would appear to give acceptably accurate results, which are also a reasonable estimate of certain spectral parameters, at least in the limited-field situation for which it was designed.

Finally, a question which may be of critical importance in the selection of a model (or models) for real-time wave forecasting purposes concerns computational speed. Considerable improvements are still to be made in the programming of all models to improve efficiency, so absolute computation times cannot yet be given. However, in relative terms it is certain that the Dexter-Bunting model is almost an order of magnitude faster than Barnett's model (and about twice as fast as that of Inoue-Bunting), and thus will probably be preferred as the forecast model on this basis alone, in view of the apparent similarity of spectral output.

Acknowledgments. I am especially indebted to F. L. Trajer, both for his valued assistance and advice throughout the course of this project, and also for supplying me with results from the Wilson-Trajer significant wave model. This paper is published by permission of the Director, Bureau of Meteorology, Australia.

REFERENCES

Barnett, T. P., 1968: On the generation, dissipation and prediction of ocean wind waves. *J. Geophys. Res.*, **73**, 513–529.

Blumenthal, R., R. Beauchesne and J. Marcus, 1967: Co-cumulative spectrum curves for the Pierson-Moskowitz (PM) spectrum. U. S. Naval Oceanographic Office, Informal Manuscript IM No. 67-2, 11 pp.

Bretschneider, C. L., 1952: Revised wave forecasting relationships. *Proc. 2nd Conference on Coastal Engineering*, Houston, Council on Wave Research, University of California.

——, 1970: Revisions in wave forecasting. *Look Lab., Hawaii*, **1**, No. 3, 31–34.

Bunting, D. C., 1966: Wave hindcast project, North Atlantic Ocean. U. S. Naval Oceanographic Office, Tech. Rept. TR-183, 36 pp.

——, 1970: Evaluating forecasts of ocean-wave spectra. *J. Geophys. Res.*, **75**, 4131–4143

Cardone, V. J., 1969: Specification of the wind distribution in the marine boundary layer for wave forecasting. New York University, Geophys. Sci. Lab., Rept. TR-69-1, 131 pp.

Darbyshire, J., 1959: A further investigation of wind-generated waves. *Deut. Hydrogr. Z.*, **10**, No. 5, 184–190.

Deacon, E. L. and E. K. Webb, 1962: Small-scale interactions. *The Sea*, Vol. 1. M. N. Hill, Ed., New York, Interscience, 43–87.

Dexter, P. E., 1973: Numerical wave generation models: I. General outline, comparison and consistency tests. Bureau of Meteorology, Australia, Tech. Rept. No. 8 (in press).

Ewing, J. A., 1971: A numerical wave prediction method for the North Atlantic Ocean. *Deut. Hydrogr. Z.*, **24**, No. 6, 241–261.

Feldhausen, P. H., S. K. Chakrabarti and B. W. Wilson, 1973: Comparison of wave hindcasts at Weather Station J for North Atlantic storm of December 1959. *Deut. Hydrogr. Z.*, **26**, No. 1, 10–16.

Gelci, R., H. Cazale and J. Vassal, 1956: Utilization des diagrammes de propagation à la prévision énergétique de la houle. *Bull. Inform. Comité Central Océanogr. Études Côtes*, **8**, No. 4, 169 pp.

Groves, G. W., and J. Melcer, 1961: On the propagation of ocean waves on a sphere. *Geofis. Intern.*, **4**, No. 1, 77 pp.

Hasselmann, K., 1960: Grundleichungen der Seegangsveroussage. *Schiffstechnik*, **7**, 191–195.

——, 1962: On the nonlinear energy transfer in a gravity wave spectrum; Part 1. General theory. *J. Fluid Mech.*, **12**, 481–500.

——, 1963: On the non-linear energy transfer in a gravity wave spectrum; Part 3. Evaluation of the energy flux and sea-swell interaction for a Neumann spectrum. *J. Fluid Mech.*, **15**, 385–398.

Inoue, T., 1967: On the growth of the spectrum of a wind-generated sea according to a modified Miles-Phillips mechanism and its application to wave forecasting. New York University, Geophys. Sci. Lab., Rept. 67-5.

Longuet-Higgins, M. S., 1952: On the statistical distribution of the heights of sea waves. *J. Marine Res.*, **11**, 245–266.

Miles, J. W., 1957: On the generation of surface waves by shear flows. *J. Fluid Mech.*, **3**, 185–204.

Neumann, G., 1952: Uber die complexe Natur des Seeganges. *Deut. Hydrogr. Z.*, **5**, 95–110.

Phillips, O. M., 1957: On the generation of waves by turbulent wind. *J. Fluid Mech.*, **2**, 417–445.

——, 1958: The equilibrium range in the spectrum of wind generated waves. *J. Fluid Mech.*, **4**, 426–434.

——, 1966: *The Dynamics of the Upper Ocean.* Cambridge University Press, 261 pp.

Pierson, W. J., 1964: The interpretation of wave spectrums in terms of the wind profile instead of the wind measured at a constant height. *J. Geophys. Res.*, **69**, 5191–5203.

——, and L. Moskowitz, 1964: A proposed spectral form for fully developed wind seas based on the similarity theory of S. A. Kitaigorodskii. *J. Geophys. Res.*, **69**, 5181–5190.

——, T. Inoue and M. S. Chang, 1965: The evaluation of a climatology of spectral wave hindcasts for a fifteen month period. Paper presented at the 46th Annual Meeting of the American Geophysical Union.

Trajer, F. L., 1966: Program NEPTUNE. Unpublished report and computer program, Bureau of Meteorology, Australia.

Walden, H., 1963: Comparison of one-dimensional wave spectra recorded in the German Bight with various theoretical spectra. *Ocean Wave Spectra*, Englewood Cliffs, N. J., Prentice-Hall, 67–81.

Wilson, B. W., 1955: Graphical approach to the forecasting of waves in moving fetches. Beach Erosion Board, U. S. Army Corps of Engineers, Tech. Memo. No. 73, 31 pp.

——, 1961: Deep water wave generation by moving wind systems. *Proc. A.S.C.E. J. Waterways Harbours Div.*, **87**, No. WW2 (Part 1), Paper 2821, 113–141.

——, 1963: Deep water wave generation by moving wind systems. *Trans. ASCE*, **128**, Paper No. 3416, 104–148.

——, 1965: Numerical prediction of ocean waves in the North Atlantic for December 1959. *Deut. Hydrogr. Z.*, **18**, 114–130.

——, S. K. Chakrabarti and P. H. Feldhausen, 1973: Hindcast of deep-water wave energy spectra for hurricane Audrey of 1957. Proc. Offshore Technology Conf., Houston, Vol. 2 (Paper OTC 1833), 121–132.